An enveloped virus-like particle vaccine expressing a stabilized prefusion form of the SARS-CoV-2 spike protein elicits highly potent immunity

Fluckiger, Anne-Catherine; Ontsouka, Barthelemy; Bozic, Jasminka; Diress, Abebaw; Ahmed, Tanvir; Berthoud, Tamara; Tran, Anh; Duque, Diane; Liao, Mingmin; McCluskie, Michael; Diaz-Mitoma, Francisco; Anderson, David E.; Soare, Catalina

Publisher's version / Version de l'éditeur:
https://doi.org/10.1016/j.vaccine.2021.07.034
Vaccine, 39, 35, pp. 4988-5001, 2021-07-16

Vaccine 39 (2021) 4988–5001

Contents lists available at ScienceDirect

Vaccine

journal homepage: www.elsevier.com/locate/vaccine

An enveloped virus-like particle vaccine expressing a stabilized prefusion form of the SARS-CoV-2 spike protein elicits highly potent immunity

Anne-Catherine Fluckiger [a,*,1], Barthelemy Ontsouka [b,1], Jasminka Bozic [b], Abebaw Diress [b], Tanvir Ahmed [b], Tamara Berthoud [b], Anh Tran [d], Diane Duque [d], Mingmin Liao [e], Michael McCluskie [d], Francisco Diaz-Mitoma [c], David E. Anderson [c], Catalina Soare [b]

[a] Bionaria, 11Bis Rue de la Garenne, 69290 Saint-Genis-les-Ollières, France
[b] VBI Vaccines, 201-310 Hunt Club Road, Ottawa, ON K1V 1C1, Canada
[c] VBI Vaccines, Cambridge, 222 Third Street, Cambridge 02142, MA, USA
[d] National Research Council Canada, Department of Human Health Therapeutics, 100 Sussex Drive, Ottawa, ON K1A0R6, Canada
[e] Vaccine and Infectious Disease Organization-International Vaccine Centre, University of Saskatchewan, 120 Veterinary Road, Saskatoon, Saskatchewan S7N 5E3 Canada

ARTICLE INFO

Article history:
Received 27 April 2021
Received in revised form 10 July 2021
Accepted 13 July 2021
Available online 16 July 2021

Keywords:
SARS-COV-2
Vaccine
Virus-like-particles
Immunogenicity
Neutralizing antibodies

ABSTRACT

We evaluated enveloped virus-like particles (eVLPs) expressing various forms of the Severe acute respiratory syndrome coronavirus-2 (SARS-CoV-2) spike protein and several adjuvants in an effort to identify a highly potent Coronavirus disease 2019 (COVID-19) vaccine candidate. eVLPs expressing a modified prefusion form of SARS-CoV-2 spike protein were selected as they induced high antibody binding titers and neutralizing activity after a single injection in mice. Formulation of SARS-CoV-2 S eVLPs with aluminum phosphate resulted in balanced induction of IgG2 and IgG1 isotypes and antibody binding and neutralization titers were undiminished for more than 3 months after a single immunization. A single dose of this candidate, named VBI-2902a, protected Syrian golden hamsters from challenge with SARS-CoV-2 and supports the on-going clinical evaluation of VBI-2902a as a highly potent vaccine against COVID-19.

1. Introduction

SARS-CoV-2 responsible for COVID-19, has been circulating worldwide for more than a year with no significant sign of natural exhaustion, in contrast to the previous Severe acute respiratory syndrome (SARS) and Middle East respiratory syndrome (MERS) epidemics in 2003 and 2012 respectively, which faded despite absence of a vaccine or specific antiviral treatments. In contrast to the SARS epidemic, the COVID-19 pandemic is associated with increasing morbidity, mortality, and mutagenic potential as more people are infected at an increasing rate [1]. Unprecedented efforts and measures have been undertaken to rapidly provide prophylactic vaccines that could decrease the rate of infection and prevent severe health complications [2].

The SARS-CoV-2 spike (S) protein was identified as a major target for neutralizing antibodies (nAb) due to its crucial role in mediating virus entry and its homology to S proteins from SARS, MERS and other CoVs for which nAb had similarly been demonstrated [3,4]. CoV protein S shares several features with class I virus fusion proteins. They are constituted of 2 functional subunits, S1, containing the receptor binding domain (RBD) and S2, containing the fusion entry domain. Binding of the RBD to the host cell receptor induces conformational changes resulting in activation of the protease cleavage site upstream of the fusion domain followed by release and activation of the S2 fusogenic domain [5]. Unlike SARS-CoV and other CoVs from the same clade, SARS-CoV-2 S contains a furin cleavage site located at the boundary of S1 and S2 [4,6]

Abbreviations: eVLP, enveloped virus-like particules; SARS-CoV-2, Severe acute respiratory syndrome- coronavirus-2; COVID-19, Coronavirus disease 2019; SARS, Severe acute respiratory syndrome; MERS, Middle East respiratory syndrome; RBD, receptor binding domain; TM-CTD, transmembrane cytoplasmic terminal domain; Ab, antibody; nAb, neutralizing antibody; MLV, murine leukemia virus; ELISA, enzyme-linked-immuno-sorbent-assay; PRNT, plaque reduction neutralization test; EPT, end-point titer; Alum, aluminum; ELISPOT, Enzyme Linked ImmunoSpot Test; IP, Intraperitoneal; IM, Intramuscular; NRC, National Research Council

* Corresponding author:
E-mail address: afluckiger@vbivaccines.com (A.-C. Fluckiger).
[1] These authors contributed equally to this work.

https://doi.org/10.1016/j.vaccine.2021.07.034
0264-410X/

enabling rapid processing of the S protein during biosynthesis in host cells.

The CoV S proteins are expressed at the viral surface as metastable prefusion trimers that undergo conformational changes [5,7]. Studies of class I viral fusion proteins resulted in the design of stabilized prefusion forms resistant to protease cleavage that could increase expression yield and elicit potent neutralization responses in mice [8,9]. Wrapp et al. [10] engineered a SARS-CoV-2 spike refered to as S-2P where two consecutive prolines in the S2 subdomain between heptad repeat 1 and the central helix were substituted with the addition of a C-terminus foldon trimerization domain. Vaccine candidates containing SARS-CoV-2 S-2P have demonstrated potent induction of nAb responses in laboratory animals [11,12] and humans [13,14]

Virus-like particles (VLPs) are attractive vaccine candidates to generate nAb responses. Structurally, they resemble the wild-type virus from which they are derived, but are much safer because they lack genetic material and therefore the ability to replicate [15]. VLPs enable repeating, array-like presentation of antigens which is a preferred means of activating B cells and eliciting high affinity antibodies [16]. Indeed, VLP expression of a B cell antigen improved neutralizing titers over 10-fold relative to immunization with the same amount of recombinant protein [17]. Accordingly, the use of VLPs as a vaccine modality may expand higher affinity B cell repertoires relative to recombinant protein or DNA/mRNA-based modalities.

In the present study, murine leukemia virus (MLV)-based enveloped virus-like particles (eVLPs) [17,18] were used to produce vaccine candidates expressing various forms of SARS-CoV-2 S. Among all constructs tested, SARS-CoV-2 S prefusion bearing the transmembrane cytoplasmic terminal domain (TMCTD) of VSV-G, refered as SPG, enabled the highest yields and density of S expression on MLV-Gag eVLPs. When adjuvanted with aluminum phosphate (Alum), SPG-eVLP induced robust and sustained nAb responses exceeding those observed with SARS-CoV-2 convalescent sera after a single dose. This formulation was selected as our vaccine candidate refered as VBI-2902a. VBI-2902a was safe and highly efficacious in a hamster challenge model after just a single dose, emphasizing the high potency of antigen expression by eVLPs.

2. Materials and Methods

2.1. COVID-19 human sera

Plasma samples were purchased from Biomex GmbH (Heidelberg, Germany). Samples were collected under consent at donation centers in Heildelberg or Munich, from 30 individuals who recovered from mild to moderate COVID-19 as defined by NIH guidelines [19]. Subjects were aged 26 to 61 years old. Sera were collected at 26 to 72 days post infection. One 61 year old woman was asymptomatic, while all others experienced mild to moderate illnesses without the need for hospitalization or oxygen supplementation. Symptoms included fever, headache, anosmia, coughing, difficulty breathing, tiredness and muscle pain.

2.2. Plasmids, eVLPs production and adjuvant formulation

Four constructs bearing SARS-CoV-2 Spike protein sequences extracted from Wuhan-Hu-1 sequence (Genbank MN908947) were designed as follows: S, unmodified full length spike protein; SG, S ectodomain fused with the TMCTD of VSV-G; SP, prefusion full length S and SPG; prefusion S ectodomain fused with VSVS-G TM-CTD (Fig. 1a). All sequences were codon optimized for expression in human cells prior to synthesis and subcloning into a proprietary modified phCMV plasmid at Genscript (Piscataway, NJ). eVLPs were produced by transient polyethylenimine transfection in proprietary HEK-293SF-3F6 GMP compliant cells provided by the National Research Council (NRC, Montreal, Canada) and grown in serum-free chemically defined medium [20]. SARS-CoV-2 S eVLPs were produced by co-transfection with one of the SARS-CoV-2 S plasmids together with a MLV-Gag plasmid as described elsewhere [18]. Control "empty" eVLPs, Gag eVLPs lacking surface expression of any form of S protein, were produced by transfection with the Gag plasmid only.

Cell culture harvests containing eVLPs were processed using a proprietary purification steps that consists of clarification, tangential flow filtration, benzonase® treatment, diafiltration and ultracentrifugation using sucrose cushion. The final product was sterile filtered using 0.2 μm membrane prior to preparation of vaccine. Depending on the pre-clinical mouse study, SARS-CoV-2 eVLPs vaccines were formulated with either Alum (Adjuphos®), MF59, or AS04 adjuvant systems purchased from Invivogen.

2.3. Western blot analysis of eVLPs content

The expression of SARS-CoV-2 S protein in eVLP preparations was analyzed by western blotting as described previously [17] using rabbit polyclonal Ab (pAb) anti-RBD of SARS-CoV-2 S (Sinobiological) followed by detection with goat anti-rabbit IgG-Fc horseradish peroxydase-conjugated (Bethyl). Alternatively, human sera from COVID-19 convalescent subjects was used as primary antibody followed by detection with goat anti-human IgG heavy and light chain HRP-conjugated (Bethyl). Precision Protein Strep-tactin HRP conjugate (Bio-Rad) was used as molecular weight ladder standard. Recombinant SARS-COV-2 S (S1 + S2) unmodified protein (Sinobiological) or SARS-CoV-2 stabilized prefusion S protein (NRC) were used as controls.

2.4. Mouse and rat immunization study

Six- to 8-week-old female C57BL/6 mice were purchased from Jackson Laboratory (ME, USA). The animals acclimatized for a period of at least 7 days before any procedures were performed. The animal studies were conducted under ethics protocols approved by the NRC Animal Care Committee. The animals were maintained in a controlled environment in accordance with the "Guide for the Care and Use of Laboratory Animals" at the NRC Animal Research facility (Institute for Biological Sciences, Ottawa, Canada). Mice were randomly assigned to experimental groups of 10–15 mice and received intraperitoneal (IP) injections with 0.5 mL of different adjuvanted SARS-CoV-2 immunogens or eVLPs produced without any spike (gag eVLPs described above). Blood was collected on day 1 before injection and day 14 after each injection for humoral immunity assessment, and spleens were colllected 14 days after the last injection for cellular immunity assessment. In some experiments, as indicated in legends, 5 mice per group, randomly picked, were sacrificed 14 days after the first injection and the remaining mice were sacrificed 14 days after the second injection. All mice from each group were sacrificed 14 days after the last immunization.

Rats study was conducted at Charles River laboratories (Laval, Canada), using 10 weeks old Wistar Han rats (Charles River Raleigh, USA) in accordance with approved ethic protocols and guide of care as mentioned above. Rats received intramuscular (IM) injections of VBI-2902a corresponding to 5 μg of S per dose.

2.5. Hamster challenge study

Syrian golden hamsters (males, 5–6 weeks old) were purchased from Charles River Laboratories (Saint-Constant, Quebec, Canada).

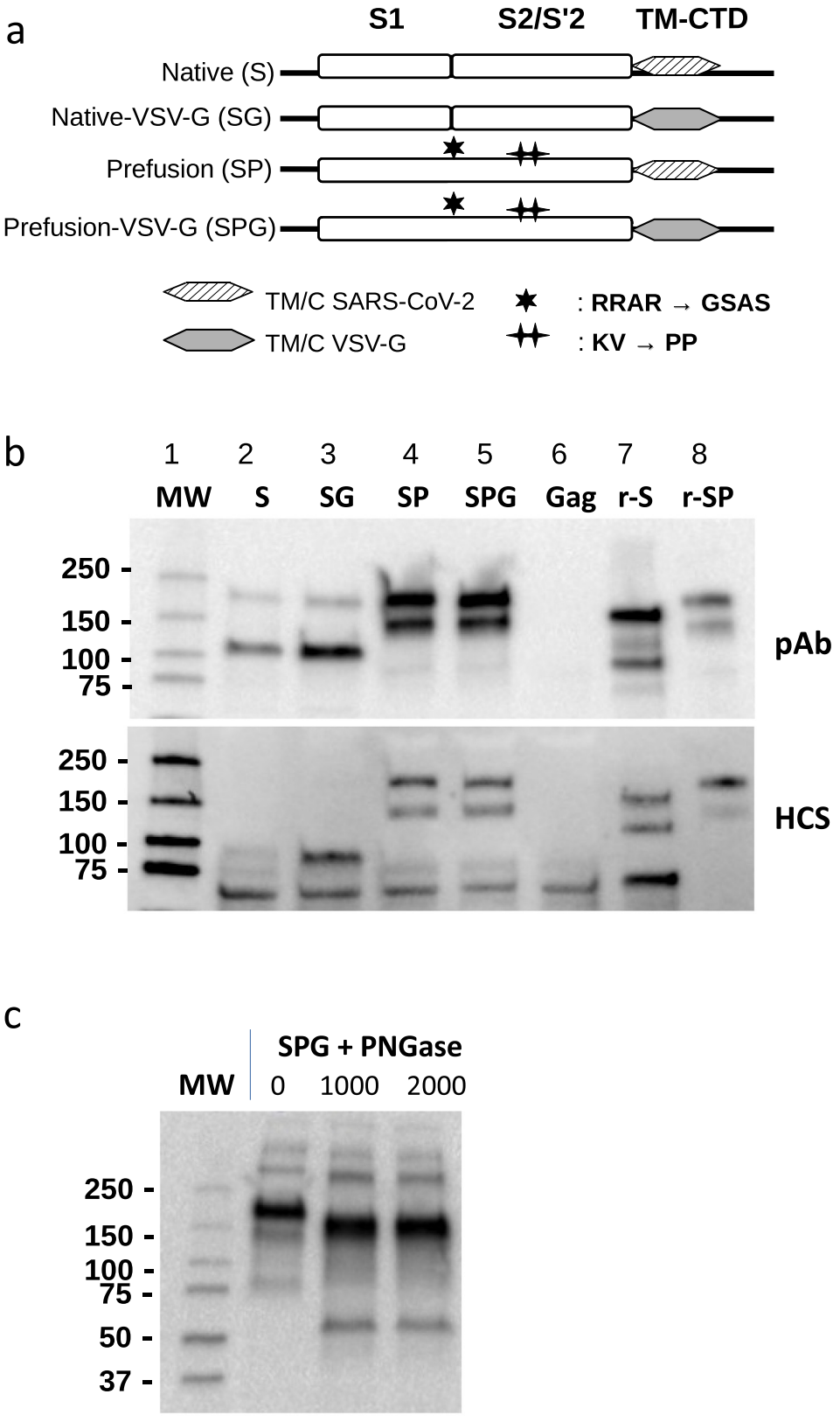

Fig. 1. Constructs design and production of eVLPs expressing SARS-CoV-2 Spike protein. (a) Schematic representation of SARS-COV-2 S plasmid constructs. TM-CTD: Transmembrane cytoplasmic terminal domain. **(b)** Expression of SARS-CoV-2 S analyzed by Western-blot of SARS-CoV-2 eVLPs and recombinant proteins using a rabbit polyclonal Ab (pAb, upper panel) raised against SARS-CoV-2 RBD (Sinobiological) or COVID-19 convalescent human serum (HuCS, bottom panel). eVLPs produced with Gag plasmid only (Gag eVLPs) and recombinant SARS-CoV-2 S proteins were used as negative and positive controls respectively. (c) Detection of SARS-CoV-2 S by Western-blot (anti-RBD pAb) after overnight incubation at 37 °C with or without PNGase F (New England Biolabs) at 1000 and 2000 Units as indicated. MW: molecular weight ladder, r-S: recombinant native S, r-SP: recombinant prefusion S protein containing a mutated furin cleavage domain (RRAR → GSAS), replacement of 2 proline (KV → PP) and a trimerization domain.

The study was conducted under approval of the CCAC committee at the Vaccine and Infectious Disease Organization (VIDO) International Vaccine Centre (Saskatchewan, Canada). Animals were randomly assigned to each experimental groups (A, B) (n = 12/group) in two independent experiments (Regimen II and Regimen I). Groups A placebo received 0.9%-saline buffer, Groups B received VBI-2902a. Each dose of VBI-2902a contained 1 μg of Spike protein and 125 μg of Alum. Injection was performed by intramuscular (IM) route at one side of the thighs in a 100 μL volume. The schedule for immunization, challenge and sample collection is depicted on Fig. 6a. All animals were challenged intranasally via both nares with 50 μL/nare containing 1×10^5 TCID50 of SARS-CoV-2/Canada/ON/VIDO-01/2020 (Sequence available at GISAID EPI_ISL_425177) strain per animal. Body weights and body temperature were measured at immunization for 3 days and daily from the challenge day. General health conditions were observed daily through the entire study period. Blood samples and nasal washes were collected as indicated on Fig. 6a. For evaluation of lung disease and RNA viral load, lung and nasal turbinates were collected after euthanazia of 6 animals per group at 3 dpi and 14 dpi. The challenge experiments were performed in the animal biosafety level 3 (ABSL3) laboratory at VIDO.

2.6. Antibody binding titers

Anti-SARS-CoV-2 specific IgG binding titers in sera were measured by standard ELISA procedure described elsewhere [17], using recombinant SARS-CoV-2 S (S1 + S2) protein (Sinobiological). For total IgG binding titers, detection was performed using a goat anti-mouse IgG-Fc HRP (Bethyl) for mouse serum, or goat anti-rat IgG Fc fragment HRP (Bethyl), or goat anti-human IgG heavy and light chain HRP-conjugated (Bethyl) for human serum. HRP-conjugated Goat anti-mouse IgG1 and HRP-conjugated goat anti-mouse IgG2b HRP (Bethyl) were used for the detection of isotype subtype. Determination of Ab binding titers to the RBD was performed using SARS-COV-2 RDB recombinant protein (Sinobiological). The detection was completed by adding 3,3′,5,5′-tetramethylbenzidine (TMB) substrate solution, and the reaction stopped by adding liquid stop solution for TMB substrate. Absorbance was read at 450 nm in an ELISA microwell plate reader. Data fitting and analysis were performed with SoftMaxPro 5, using a four-parameter fitting algorithm.

Ab binding titers in hamster sera were determined with ELISA method. Plates were coated with spike S1 + S2 Ag (Sinobiological). The coating concentration was 0.1 μg/mL. Plates were blocked with 5% non-fat milk powder in PBS containing 0.05% Tween 20. Four-fold dilutions of serum were used. Goat anti-Hamster IgG HRP from ThermoFisher was used as the secondary antibody at 1:7000. Plates were developed with OPD peroxidase substrate (Thermo Scientific Pierce). The reaction was stopped with 2.5 M sulfuric acid and absorbance was measured at 490 nm. Throughout the assay, plates were washed with PBS containing 0.05% Tween 20. The assay was performed in duplicate. The titers were reported as the end point titer corresponding to the first dilution that gave an OD 3-fold higher than the background.

2.7. Virus neutralization assays

Neutralizing activity in mouse serum samples was measured by standard plaque reduction neutralization test (PRNT) on Vero cells at the NRC using 100 PFU of SARS-CoV-2/Canada/ON/VIDO-01/2020. Results were represented as PRNT90, PRNT80, or PRNT50 end point titer, corresponding to the lowest dilution inhibiting respectively 90% or 80% or 50% of plaque formation in Vero cell culture.

Virus neutralization assays against the challenge SARS-CoV-2 virus were performed at VIDO, on the hamster serum samples collected at pre-challenge and at the end day; 3 days post-challenge or 14 days post-challenge. The study was conducted using the cell line Vero E6. The serum samples were heat-inactivated for 30 min at 56 °C. The serum samples were initially diluted 1:10 and then serially diluted (2-fold serial dilutions). The virus was diluted in medium for a final concentration of 3×10^2 TCID50/mL. Initially 60 μL of the virus solution was mixed with 60 μL serially diluted serum samples. The mixture was incubated for 1hr at 37 °C, with 5% CO2. The pre-incubated virus-serum mixtures (100 μL/well) were transferred to the wells of the 96-well flat-bottom plates containing 90% confluent pre-seeded VeroE6 cells. The plates were incubated at 37 °C, with 5% CO2 for 5 days. The plates were observed using a microscope on day 1 post-infection for contamination and on days 3 and 5 post-infection for cytopathic effect (CPE). The serum dilution factor for the last well with no CPE at 5 dpi was defined as the serum neutralization titer. The initial serum dilution factor was 1:20.

2.8. Viral pRT-PCR on hamster RNA

Extraction of RNA from lung (cranial and caudal lobes) and nasal turbinates was completed using approximately 100 μg of tissue. The tissues were homogenized in 600 μL of lysis buffer (RLT Qiagen) with a sterile stainless steel bead in the TissueLyserII (Qiagen) for 6 min, at 30 Hz. The solution was centrifuged at 5000 × g for 5 min. Supernatant was transferred to a fresh tube containing 600 μL of 70% ethanol, and the tube was incubated at room temperature for 10 min. Viral RNA was then purified using Qiagen Rneasy Mini Kit (Cat No /ID: 74106) and eluted with 50 μL elution buffer.

The qRT-PCR assays were then performed using SARS-CoV-2 specific primers targeting the *env* gene of SARS-CoV-2 (Fwd, *ACAGGTACGTTAATAGTTAATAGCGT;* Rev, *ATATTGCAGCAGTACGCACACA*) and labelled probe, *ACACTAGCCATCCTTACTGCGCTTCG*. The primers have an annealing temperature of approximately 60 °C. Qiagen Quantifast RT-PCR Probe kits were used for qRT-PCR. The qRT-PCR results were expressed in RNA copy number per reaction. This was done by producing a standard curve with RNA extracted from a sample of SARS-CoV-2 which was cloned to determine exact copy number of the gene of interest. The Ct values for individual samples were used with the standard curve to determine the copy number in each sample. The qRT-PCR reactions were performed using the OneStepPlus (Applied Biosystems) machine. The program was set at: Reverse transcription (RT) 10 min at 50 °C; Inactivation 5 min at 95 °C; and then 40 cycles of denaturation for 10 sec at 95 °C and annealing/extension for 30 sec at 60 °C.

2.9. IFN-γ Ex-vivo ELISPOT

IFN-γ ELISPOT analyses to measure Th1 T cell responses were performed as follows. One day before the spleens were removed, ELISpot plates (Millipore) were coated with IFN-γ capture antibody at a concentration of 15 μg/mL (Mabtech). The following day, mice were sacrificed and spleens were removed. Spleens from individual mice were processed to produce single cell suspensions. Erythrocytes were lysed using a commercially available RBC lysis buffer (BioLegend). Fifty microliters containing $2x10^6$ splenocytes were then to each well of a pre-blocked ELISPOT plate. Then, fifty microliters of stimulant pepmixes (JPT peptides) resuspended in RPMI + 10 % FBS (R10) with recombinant mouse IL-2 (rmIL-2) (R&D Systems) were added to each well. The final concentration of each peptide in the assay was 1 μg/mL/peptide, and the final concentration of rmIL-2 was 0.1 ng/mL. R10 alone was used as a negative control and PMA + Ionomycin as a positive control. The ELISPOT plates were then placed into a humid 37 °C with 5% CO2 incubator for 40–48 h. After incubation, the plates were washed

and IFN-γ capture antibody was added, followed by streptomycin horseradish peroxidase (strep-HRP). The plates were developed with commercially available 3-Amino-9-ethylcarbazole (AEC) substrate (Sigma-Aldrich). The observed spots were counted using an ELISPOT plate reader by ZellNet and the final data was reported as spot forming cells (SFC) per one million splenocytes.

2.10. Histopathology

At necropsy the left lung of hamsters was perfused with neutral-buffered formalin immediately after collection. Tissues were fixed in neutral-buffered formalin for a week, then placed into fresh neutral-buffered formalin before being transferred from containment level 3 to containment level 2 laboratory. Tissues were embeded, sectioned and stained with hematoxylin and eosin. Slides were examined by a board-certified pathologist.

2.11. Statistics

All statistical analyses were performed using GraphPad Prism 9 software (La Jolla, CA). Unless indicated, multiple comparison was done with Kruskall-Wallis test. The data were considered significant if $p < 0.05$. Geometric means (geomean) with standard deviation are represented on graphs. No samples or animals were excluded from the analysis. Randomization was performed for the animal studies.

3. Results

3.1. Impact of SARS-CoV-2 S antigen design on expression and yield

Four constructs were designed based on the spike protein sequence of the SARS-CoV-2 Wuhan-Hu-1 isolate and subcloned into expression plasmids for the production of eVLPs as described in Methods (Fig. 1a). To obtain a stabilized prefusion form of S (SP), the furin cleavage site of S, RRAR, was inhibited by mutation of the 3 arginines into a glycine and 2 serine (GSAS) and 2 proline substitutions were introduced at successive residues K986 and V987. Our previous work has demonstrated that the swap of the transmembrane cytoplasmic terminal domain (TMCTD) of CMV glycoprotein B resulted in enhanced yields and immunogenicity of the gB glycoprotein presented on eVLPs [17]. Based on this data, two additional constructs, Native-VSVg (SG) and Stabilized Prefusion-VSVg (SPG) were designed by swapping the TMCTD of S with that of VSV-G. The resulting four types of eVLPs were analysed by Western blot using a polyclonal Ab directed against the SARS-CoV-2 S receptor binding domain (RBD) and human convalescent serum. The eVLPs produced with S and SG constructs showed two major bands around 180 KDa and 100 KDa corresponding to the full length and cleaved S proteins as previously demonstrated [21] (Fig. 1b, lane 2–3). In contrast, eVLPs produced with SP and SPG constructs expressed only the uncleaved full length 180 KDa protein as the result of the furin cleavage site mutations. Expression of S was slightly improved by the VSV-G swap in SG, and more dramatically enhanced by the inhibition of the cleavage sites in SP and SPG (Fig. 1b, lane 4–5). An additional band around 150 kDa was reproducibly observed upon overexpression of uncleaved S. Results from deglycosylation experiments suggested that it reflected S protein deprived of N-Glycosylation (Fig. 1c), as already described with recombinant S [22], and that would occur because of overloading of the host cell machinery. Similar results were obtained after blotting with human convalescent serum (Fig. 1b).

Quantitative analysis of protein content in eVLP preparations showed that for a similar number of particles and comparable amounts of Gag protein, the amount of SARS-CoV-2 S protein was increased substantially with replacement of the TMCTD and by use of the stabilized prefusion construct, suggesting that the density of the S protein was enhanced using the VSV-G constructs (Table 1). The best yield was reproducibly obtained when producing the eVLPs expressing the prefusion VSV-G form of S, with up to a 40-fold increase relative to eVLPs expressing native S.

3.2. Impact of SARS-CoV-2 S antigen design on neutralizing antibody responses

Comparison to convalescent serum is commonly used as a benchmark to help evaluate immunogenicity and potential efficacy of Covid-19 candidate vaccines. However, a wide spectrum of Ab responses can be observed in recovering patients, ranging from barely detectable to very high levels, likely influenced by time since infection and severity of disease. To enable comparison across experiments, we obtained a cohort of 20 sera from COVID-19 confirmed convalescent patients with moderate COVID-19 symptoms who all recovered without specific treatment intervention or hospitalization. The cohort was separated into two groups of 10 samples according to high or low levels of Ab binding activity to SARS-CoV-2 (Suppl. Fig. 1a-b, [23]). Sera from each group were then pooled and tested for neutralizing activity (Suppl. Fig. 1c). As expected, the pool of human sera showing higher levels of IgG titers against SARS-CoV-2 S had the highest neutralizing activity, which was consistent with previous observations [24]. To provide a robust benchmark with which to assess the immunogenicity of the vaccine candidates, only the high titer pooled sera was used to assess vaccine-induced responses in animals.

Humoral responses of the various types of SARS-CoV-2 eVLPs and control eVLPs devoid of Spike protein were evaluated in C57BL/6 mice that received 2 IP injections at 3 week intervals (Fig. 2). In mice, VLP immunization induces comparable humoral responses after IP and IM administration [25], but the IP route is prefered to IM because of the small size of the muscles and comparatively large volume when using alum-based formulations. No Ab binding against SARS-CoV-2 S and no neutralization activity against SARS-CoV-2 virus could be detected in sera from control group diluted 1/100 either tested as pools (Fig. 2a-b) or as individual sera (not shown). The first injection of unmodified S presented on eVLPs induced levels of anti-SARS-CoV-2 S Ab binding titers similar to those in mice that received a recombinant trimerized prefusion S protein, but they were not associated with significant (90% or greater) neutralization activity as measured in a plaque reduction neutralization test (PRNT) (Fig. 2a-b). In contrast, a significant nAb response was induced by a single injection of eVLPs expressing prefusion SP or SPG, with PRNT90 end-point titers (EPTs) of 80 and 160 respectively. These values were higher than

Table 1
Optimisation of SARS-CoV-2 S protein yields by alteration of the sequence construct.

Spike Construct	Gag total amount (mg)	SARS-CoV-2 S total amount (mg	S to Gag ratio (%)	Particle number/mL
Native (S)	23	0.16	0.7	4.37×10^{11}
Native-VSV-G (SG)	19	0.5	2.63	4.37×10^{11}
Prefusion (SP)	32	0.23	0.72	4.37×10^{11}
Prefusion-VSV-G (SPG)	23	0.64	2.78	4.37×10^{11}

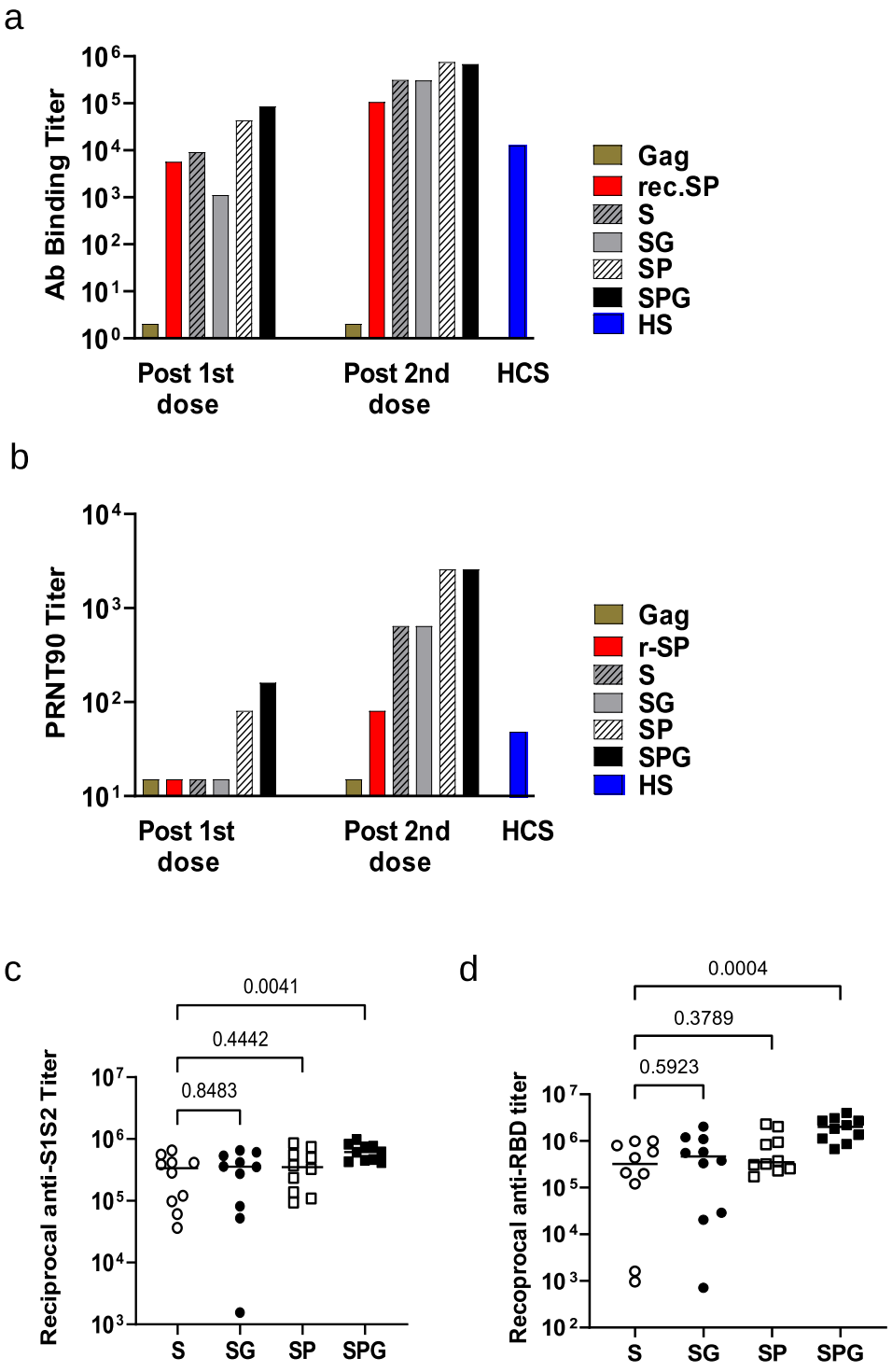

Fig. 2. Immunogenicity of the various forms of SARS-CoV-2 S eVLPs in C57BL/6 mice. C57BL/6 mice, 10 per group, received 2 injections of Gag eVLPs deprived of S or various forms of SARS-CoV-2 S or recombinant prefusion SP at day 0 and 21 as indicated on legend, S: native S, SG: S with VSV-G tail, SP: prefusion S, SPG: prefusion S with VSV-G tail, r-SP: recombinant SP protein. Sera were collected 2 weeks after each injection. **(a)** Pooled sera from each group were analyzed for specific SARS-CoV-2 S (S1 + S2) total IgG; results are represented as EPT corresponding to the first dilution that gave an OD 3-fold above background. **(b)** Pooled sera from each group were analyzed in PRNT assay with a 90% threshold (PRNT90) as described in Material and Methods. A pool of human sera from COVID-19 convalescent patients with moderate disease (HCS) was used as reference. **(c-d)** Individual sera were analyzed in ELISA using recombinant SARS-CoV-2 S (S1 + S2) protein (c) or recombinant SARS-CoV-2 RBD protein (d). All 10 sera from Gag eVLP control group were negative in the same ELISA at PRNT at dilution of 1/500 and were not represented in fig. c and d. P values from Kruskall-Wallis test comparing groups are indicated in c and d. Serum from mice that received the negative control eVLP deprived of S were below the detection limit in both S1S2 and RBD ELISA and were not represented on graphs c and d.

those observed with the human convalescent control pool (PRNT90 EPT of 50). All nAb responses were greatly enhanced by the second injection and reflected the responses that were observed prior to the boosting dose. Notably, all forms of SARS-CoV-2 S presented on eVLPs induced higher antibody titers than recombinant prefusion S protein, both in the levels of total IgG and neutralization activity, after one or two injections.

Individual mice sera obtained 14 days after the second injection of eVLPs were evaluated for the specificity of the Ab responses against the whole S1 + S2 protein or the RBD (Fig. 2c-d). All

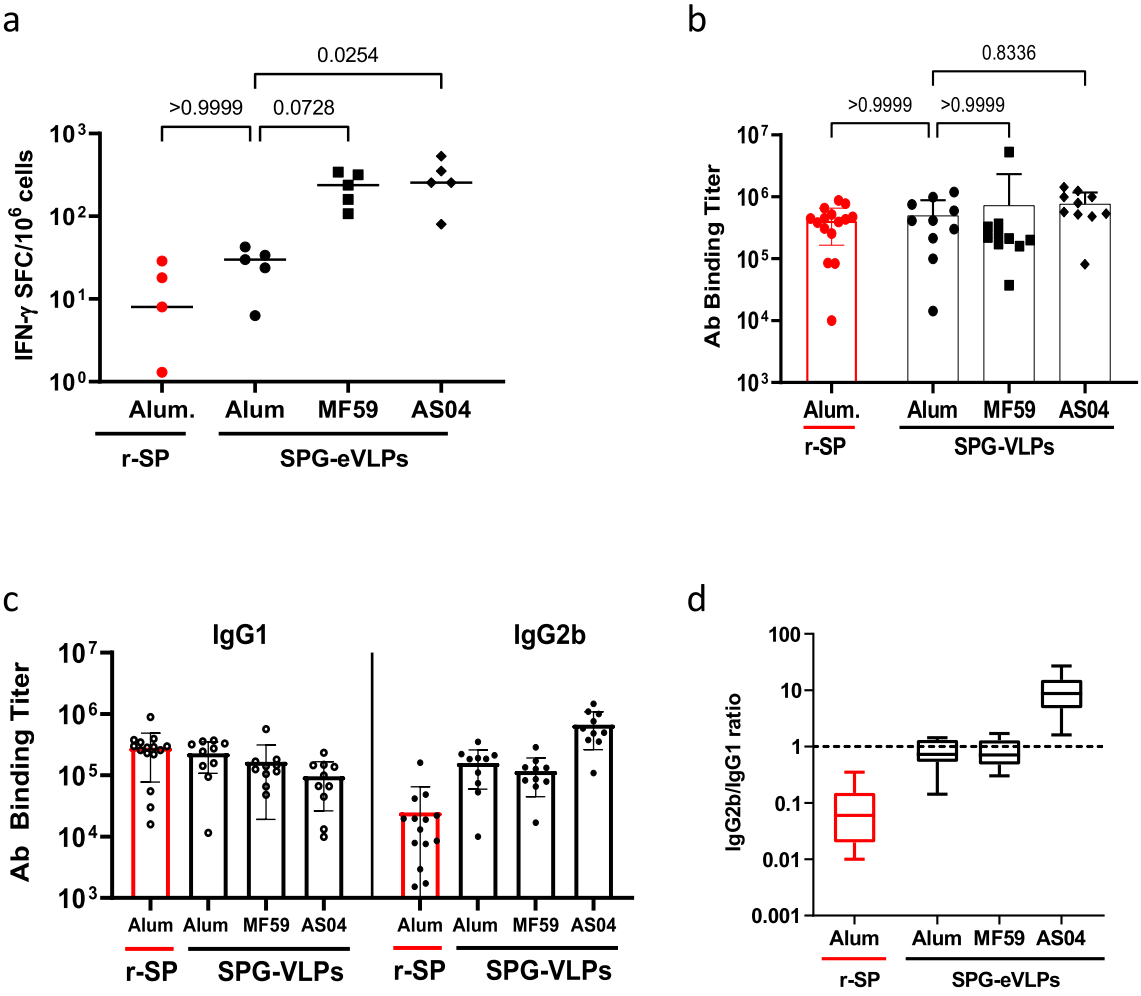

Fig. 3. Influence of various adjuvants in the SARS-CoV-2 S eVLPs-mediated Ab and T cell response. At day 0 and 21, five groups of 10 C57BL/6 mice received 2 injections of S eVLPs in the presence of various adjuvants as indicated in legends and described in Material and Methods. Sera and splenocytes were collected 2 weeks after the second injection. **(a)** Numbers of IFNγ producing cells per million splenocytes collected from 5 mice randomly picked 2 weeks after the second injection were measured by ELISpot using peptide pool covering the entire S(S1 + S2) protein. **(b)** Total IgG were measured in ELISA against recombinant SARS-CoV-2 S (S1 + S2) protein, results are represented as EPT. **(c-d)** Isotype usage was determined in individual sera by specific ELISA using HRP conjugate goat Ab against mouse IgG1 and IgG2. (c) Results are expressed as the ratio of IgG2b to IgG1. Results from Kruskall-Wallis comparison of groups are indicated.

immunized mice that received eVLPs showed robust anti-SARS-CoV-2 Ab responses either against a full length S1 + S2 protein (Fig. 2c) or against the RBD protein (Fig. 2d). A more homogenous response was observed in mice that received the SPG eVLPs, with all Ab EPTs above 400,000 against S (5.6 Log 10), and above 650,000 against RBD (5.8 Log10).

3.3. Influence of adjuvants on antibody and T cell responses

Aluminum salts are commonly used adjuvants in the formulation of VLP-based vaccines against hepatitis B (e.g. Engerix-B®) or human papillomavirus (e.g. Gardasil®) with an extensive safety record. However, they have also been demonstrated to induce Th2 biased antibody and T cell responses in some instances, which could be detrimental for a SARS-CoV-2 vaccine. Indeed, a Th2-type response has been suggested to contribute to the "cytokine storm" associated with vaccine-induced severe lung pathologies [26,27]. Therefore, we compared formulation of eVLPs with Alum to MF59 and the adjuvant system AS04. Native S eVLPs were prefered for this experiment because they induced suboptimal nAb responses compared to SPG eVLPs and enabled the potency of each adjuvant to enhance immunogenicity to be better appreciated. The various adjuvanted formulations of S eVLPs were compared to recombinant stabilized prefusion S protein (r-SP) formulated in Alum adjuvant, which was expected to induce a Th2-biased response [28]. Mice received two IP injections and Ab and T cell responses were measured 14 days after the second injection (Fig. 3). MF59 enhanced IFN-γ T cell responses compared to Alum (Fig. 3a) but induced similar Ab responses (Fig. 3b-c) and a comparable, balanced IgG2/IgG1 ratio (Fig. 3d). The AS04 adjuvant skewed responses towards a Th1-type T cell response. Most remarkably, while r-SP in Alum preferentially induced IgG1 Ab representative of a Th2 response, S-eVLPs induced balanced production of IgG1 and IgG2b indicating a balanced Th1/Th2 response (Fig. 3d). As formulation in Alum induced a balanced Th1/Th2 response rather than a strong Th2 skewed response, and because of its extensive record of clinical safety, we chose Alum as the adjuvant of choice for our VLP candidate vaccine against SARS-CoV-2.

3.4. Immunogenicity in mice of vaccine candidate VBI-2902a

While prefusion spike SP eVLPs and modified prefusion SPG eVLPs induced comparable levels of neutralizing Ab responses, yields of SPG eVLPs productions were reproducibly higher than those of SP eVLPs or any other constructs. Based on these results above, we chose to evaluate the immunogenicity and potential

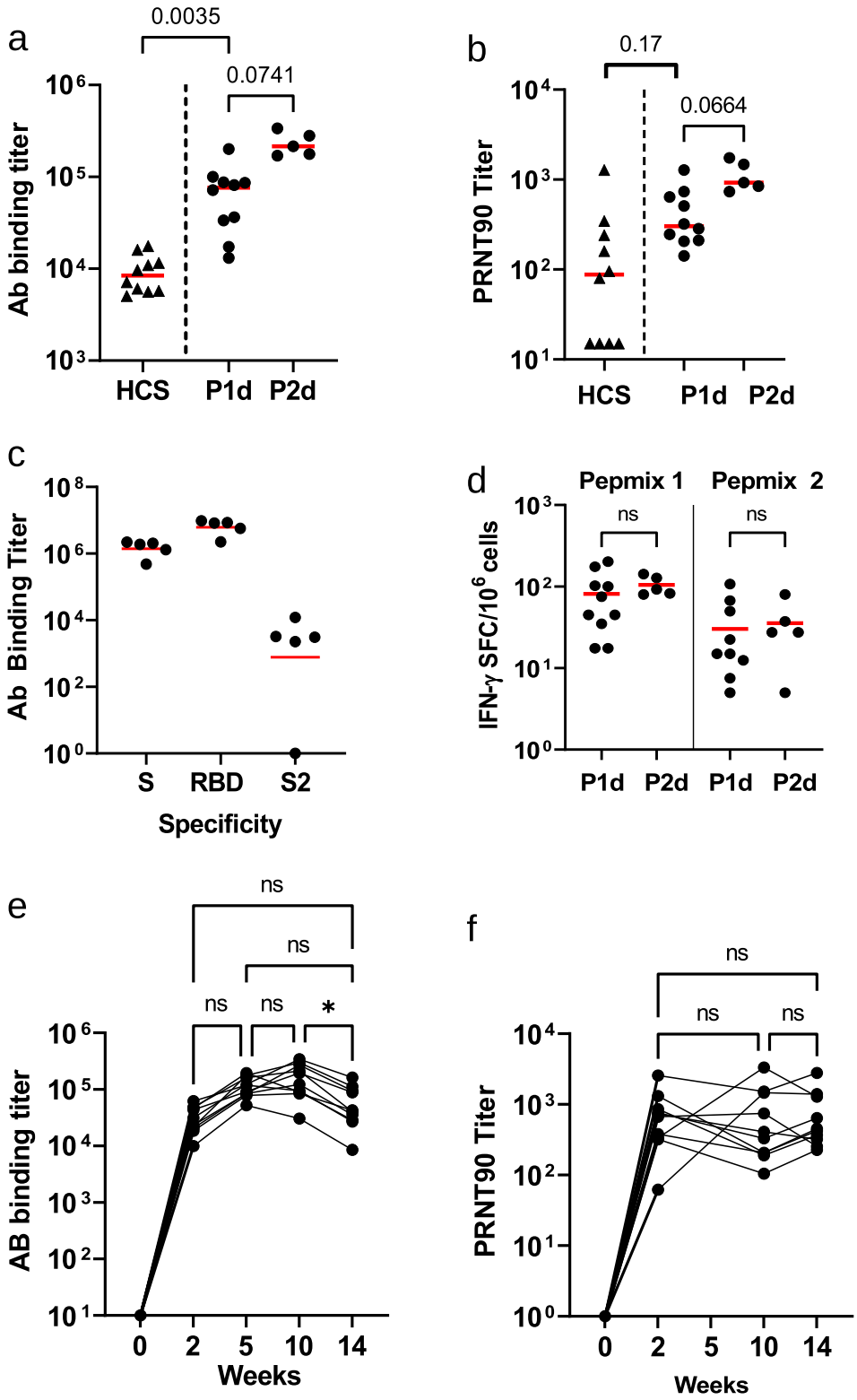

Fig. 4. Immunogenicity of VBI-2902a in C57BL/6 mice. (a-d) Two groups of 10 mice were immunized twice at 3 weeks interval with VBI-2902a containing 0.2 μg of S protein. Blood was collected 2 weeks after each injection, P1d: post 1st dose, P2d: post 2nd dose. **(a)** Ab binding titer against recombinant S (S1 + S2) compared to human convalescent sera, measured by ELISA, **(b)** neutralization end point titers measured by PRNT90, **(c)** Ab binding titers against recombinant S(S1 + S2), recombinant RBD or recombinant S2 measured by ELISA in sera after the 2nd dose. Results from Kruskall-Wallis comparison of groups are indicated for a and b. **(d)** Numbers of IFN-γ producing cells per million splenocytes collected 2 weeks after each injection were measured by ELISpot using Pepmix 1 or Pepmix 2 preferentially covering SARS-CoV-2 S1 domain or S2 domain respectively. **(e, f)** Kinetic of the humoral response after single injection of VBI-2902a calculated as end point titer determined in ELISA (e) and PRNT90 (f). Each dot represent individual animal serum. Paired, non parametric, Friedman test with Dunn's correction for multiple comparison was performed to compare values between time points; a p value of $\leq$ 0,05 was considered statistically significant.

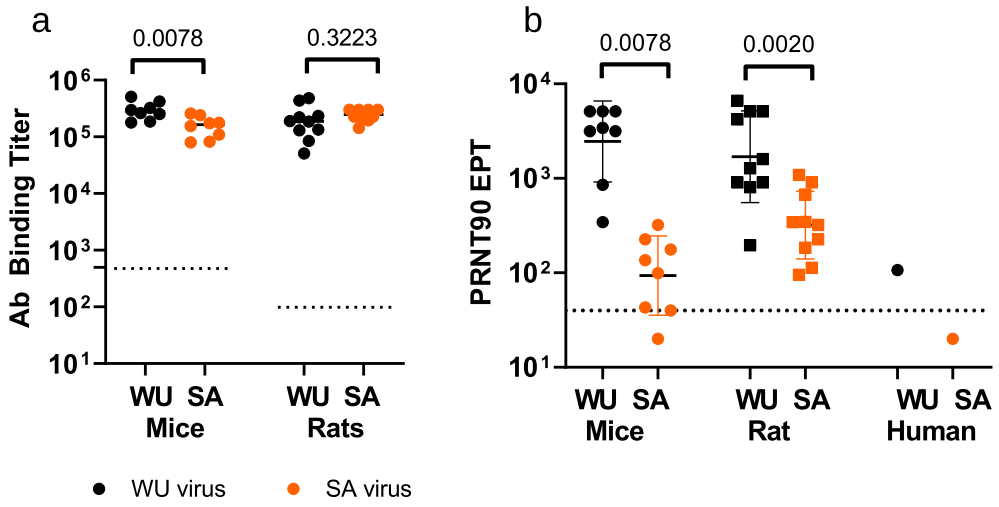

Fig. 5. Crossreactivity induced by VBI-2902a on SARS-CoV-2 B.1.351 variant. Two groups of 8 mice received 2 injections of VBI-2902a or Gag eVLPs and two groups of 10 rats received 2 injections of VBI-2902a or Saline. Blood samples were collected 14 days after the second injection for monitoring of humoral responses. (**a**) Ab binding titers measured by ELISA using WU recombinant spike protein and SA variant recombinant spike protein as described in Material and Methods. All mouse sera from the Gag control group were negative at the first dilution tested of 1/500 and all rat sera from Saline control groups were negative above 1/100 dilution. These control values were represented by a doted line. (**b**) PRNT90 were performed as described in Material and Methods with either SARS-CoV-2 lineage B, hCOV-19/Canada/ON-VIDO-01/2020 (WU) or lineage B.1.351, hCOV-19/SouthAfrica/KRISP-EC-K005321/2020 (SA) viruses. GM with GM standard deviation are represented. A pool of COVID-19 convalescent human plasma samples (HCS) collected before emergence of the SA variant was also tested in PRNT90.The doted line represent the base line of the assay corresponding to the last dilution of 1/40. Values below this baseline indicated that no cytopathic effect was detected at the 1/40 dilution. Statistical analysis was performed with non parametric unpaired T test (Wilcoxon tests).

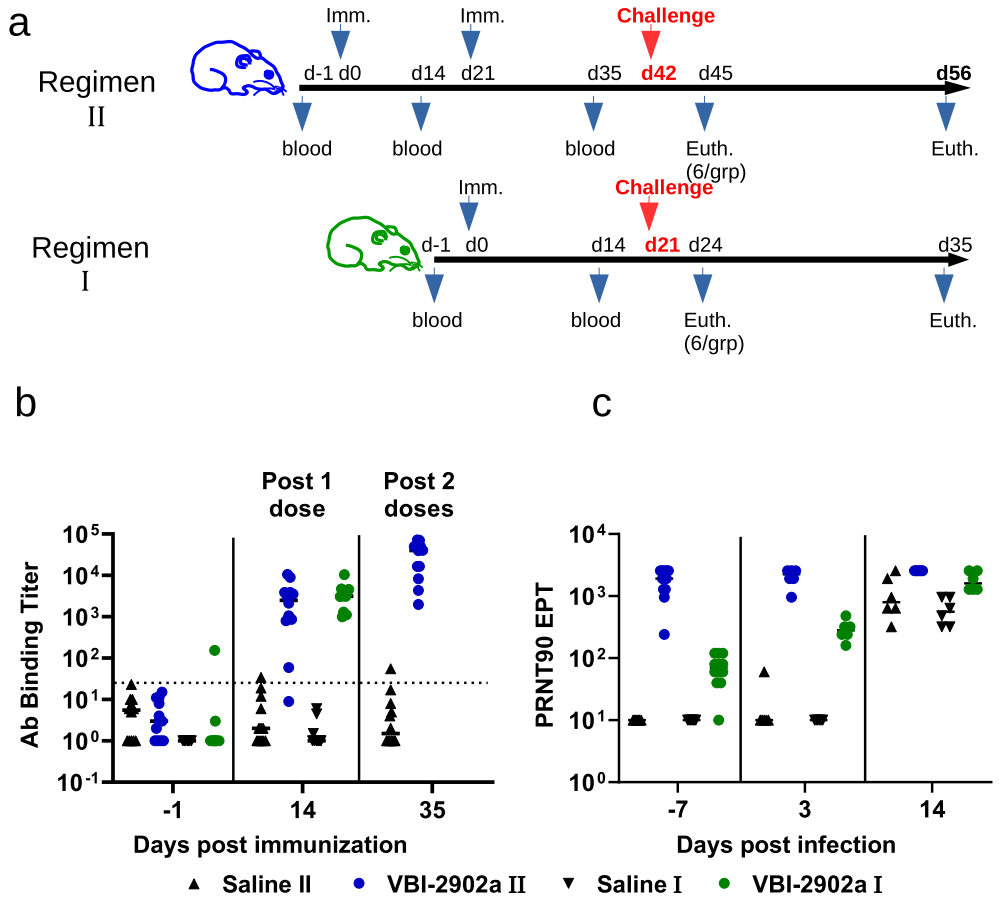

Fig. 6. Immunogenicity of VBI-2902a in Syrian gloden hamsters. (a) Schematic representation of the challenge experiments. Each challenge experiment used 2 groups of 12 Syrian gold hamsters. In regimen II, animals received 2 IM injections of VBI-2902a (1 μg of S per dose) or placebo saline buffer administered at 3 weeks interval. In regimen I, animals received a single injection of VBI-2902a or Saline buffer. Blood was collected 2 weeks after each injection. Three weeks after the last injection corresponding to day 42 in regimen II and day 21 in regimen I, hamsters were exposed to SARS-CoV-2 at $1x10^5$ TCID50 per animal via both nares. At 3 days post infection (dpi), 6 animals per groups were sacrificed for viral load analysis. The remaining animals were clinically evaluated daily until end of study at 14dpi. **(b)** Anti-SARS-CoV-2 S(S1 + S2) total IgG EPT measured by ELISA 2 weeks after each immunization. **(c)** Neutralization activity was measured by PRNT90 in immunized groups; results are represented as PRNT90 EPT.

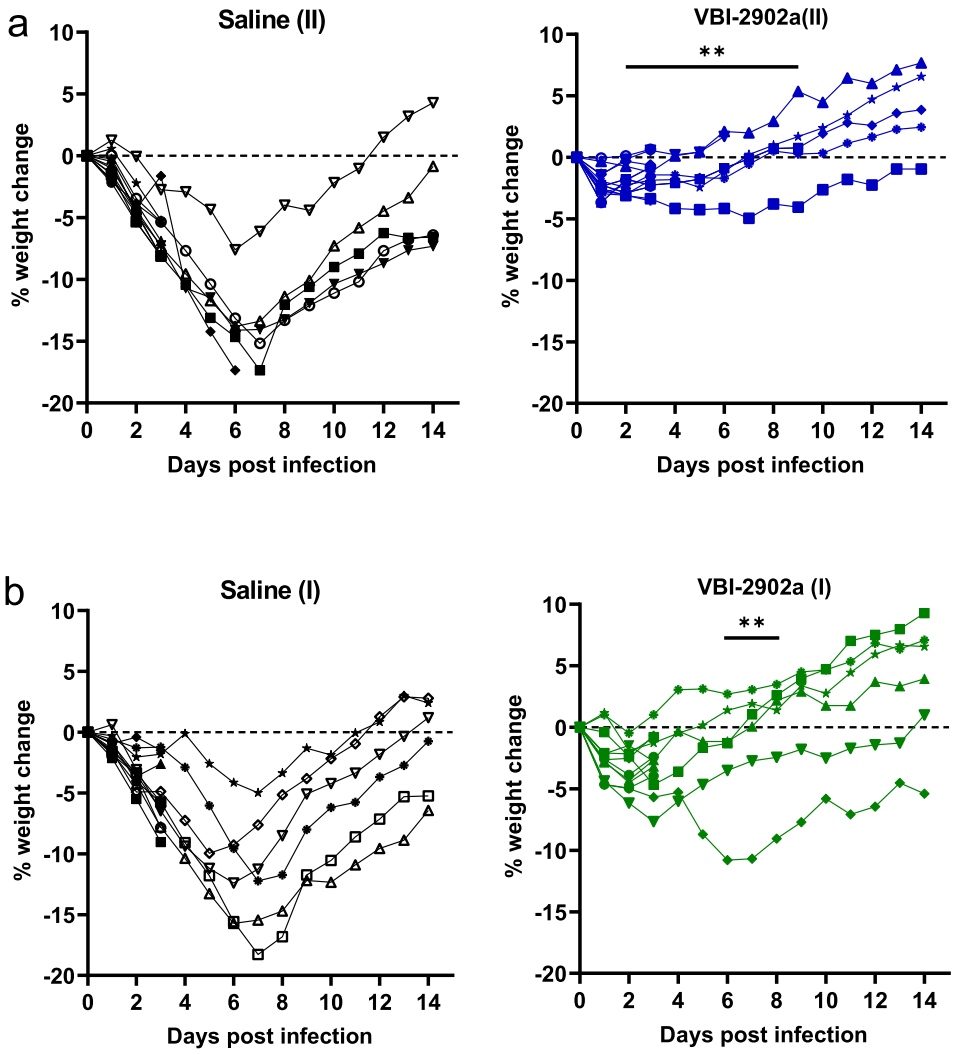

Fig. 7. Weight change of hamsters after exposure to SARS-CoV-2. Hamsters from experiment described in Fig. 6 were monitored daily for weight change. Results are represented for each animal in each groups as kinetic of weight change from SARS-CoV-2 exposure to day 9 after infection. **(a)** represents the weight change observed in the 2-dose regimen (II), **(b)** represent the weight change observed in the single dose regimen (I). One animal from Saline group II and one animal from VBI-2902(II) were sacrificed at day 6 and day 7 respectively, because they presented intense distress. Animal from Saline(II) presented typical clinical signs of SARS-CoV-2 infection. Severe clinical presentation of animal in VBI-2902a(II) could not be related to SARS-CoV-2 infection and have not been determined. Significant days of weight loss relative to Saline group ($p < 0.005$) are indicated on the left panel. Statistical analysis was performed with unpaired non parametric multiple *t* test using Holm-Šidák method.

efficacy of eVLPs expressing SPG protein formulated with Alum, named VBI-2902a, after one or two injections 21 days apart. Fourteen days after a single injection, sera from mouse immunized with VBI-2902a contained total anti-Spike IgG EPTs reaching geometric means of (4.8 Log10) 54,891 that were associated with neutralizing PRNT90 titers of 365 (2.6 Log10). A second injection boosted Ab binding titers to 228,374 (5.4 Log10) with nAb titers of 1,079 (3.0 Log10) (Fig. 4a-b). Levels of nAb response were higher than those observed in sera from convalescent patients. Abs were preferentially directed against the RBD and S1 with only low binding to S2 (Fig. 4c).

Mouse splenocytes collected 2 weeks after each immunization were stimulated *ex vivo* using two different peptide pools preferentially covering the S1 domain (pepmix 1) or the S2 domain (pepmix 2) respectively. Numbers of IFN-γ spot forming cells (Fig. 4d) suggested preferential T cell responses against the S1 domain of the spike protein rather than against the S2 domain. No major increases in T cell responses were observed after the second injection of VBI-2902a.

Additionally, in mice, a single dose of VBI-2902a induced a sustained Ab response for at least 15 weeks without any drop in neutralization titers (Fig. 4e-f) despite a slow decrease of Ab titers after 10 weeks.

Sera from both mice and rats that had received 2 injections of VBI-2902a were used to assess the crossreactivity of VBI-2902a induced humoral immunity against B.1.351 "South Africa" variant (SA). High antibody binding crossreactivity against WU and SA recombinant spike proteins was observed (Fig. 5a) with geomean titers of 285,794 (WU) vs. 146,369 (SA) in mice (Willcoxon test p 0.0078, n = 8) and 175,748 (WU) vs 240,034 (SA) in rats (Wilcoxon test p value of 0,3223, n = 10). However, the high levels of neutralization activity measured in PRNT90, (geoman of 2458 in mice and 1694 in rats) significantly dropped against the SA variant with geomean of 94 in mice and 320 in rats) (Fig. 5b).

3.5. Protective efficacy of VBI-2902a in Syrian golden hamsters

The protective efficacy of VBI-2902a was examined in Syrian Gold hamsters. SARS-CoV-2 infection in Syrian Gold hamsters resembles features found in humans with moderate COVID-19 and is characterized by a rapid weight loss starting 2 days post infection (dpi) [29,30]. Two immunization regimens were

compared. Regimen II consisted of two IM injections of VBI-2902a or saline at 3 weeks interval whereas Regimen I consisted of a single dose injection of VBI-2902a or saline (Fig. 6a). Three weeks after the last injection (day 42 in Regimen II and day 21 in Regimen I), all animals were inoculated intranasally with 1×10^5 TCID50 of SARS-CoV-2 per animal and monitored daily for weight change, general health and behavior.

After a single injection of VBI-2902a the levels of anti-S IgG rapidly increased in the serum of immunized animals with EPTs reaching $1\text{-}2x10^3$ (Fig. 6b). The second injection enhanced these levels approximately 10-fold to reach EPTs of $2\text{-}3x10^4$ at day 35, which translated into robust neutralization titers of over 10^3 EPT as measured by PRNT90 (Fig. 6c). In the single dose regimen, the neutralization activity (geomean of 69), was increased 250-fold to 1725 within 3 days after exposure to the virus.

Animals in all groups lost 2–4% of body weight 2 days post infection (2dpi) (Fig. 7a-b). Animals in the saline control groups continued to lost weight until an average 15% loss at 7dpi at which time 11 of 12 began to regain weight. One animal was euthanized at 7 dpi because of a severe clinical presentation associated with a loss in weight. Histophathology at necropsy revealed severe lung pathology (score of 4 with inflammation and cell infiltration). In marked contrast, none of the hamsters immunized with two doses of VBI-2902a lost any further weight after 2dpi, regaining normal weight by 7dpi (Fig. 7a). In group VBI-2902a(II), one animal that had regained its weight at 3 dpi was found moribond and was euthanized. Its clinical condition was not associated with lung pathology. In the single dose regimen, the majority of the animals started to regain weight after 3dpi instead of 2dpi (Fig. 7b). Statistical analysis indicated a significant difference in body weight loss between control groups and vaccinated groups from day 2 to day 9 after two doses and from day 6 to day 8 after one dose.

At 3dpi, two doses of VBI-2902a resulted in highly significant (p = 0001) viral load median reductions (Fig. 8a) of 4,45 Log10 (IQR 4,95–4,33)in the cranial lobe and 5,17 Log10 (IQR 5,69–4,39) in the caudal lobe relative to non-immunized animals. A Significant decrease of viral RNA was also observed after a single dose of vaccine with median decreases of 2,28 Log10 (IQR 2,68–2,06) in the cranial lobe and 3,49 Log10 (IQR 3,61–3,42) in the caudal lobe. The viral load values observed in lungs were inversely correlated with the neutralization measured as PRNT90 (Fig. 8b-c). More viral RNA was found in nasal turbinates, which may have included residual viral inoculum as suggested previously [30,31]. Data from prior studies also suggested an extended persistence of the virus in nasal turbinates while bearly detectable in the lung [29]. Both vaccine regimens induced decreases in lung-to-body weight ratio (Fig. 9a) and in lung histopathological scores (Fig. 9b) compared to Saline controls. However, higher statistical differences observed with the two-dose regimen suggested that the 2 doses of VBI-2902a induced better protection than the single dose.

4. Discussion

The unprecedented urgency for a safe COVID-19 vaccine that can confer protection as quickly as possible with as few doses as

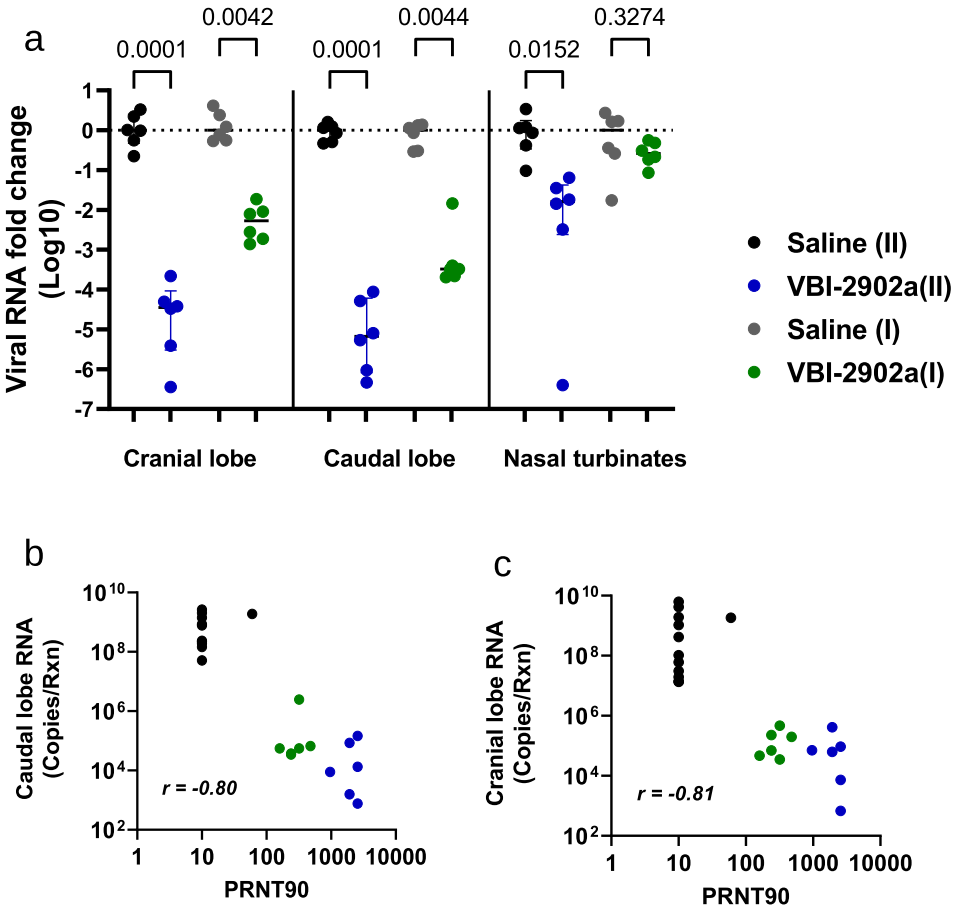

Fig. 8. Viral load analysis in SARS-CoV-2 infected hamsters. (a-b) At 3dpi, qRT-PCR assays were performed on RNA from samples of nasal washes, lung tissues (cranial and caudal lobes) using SARS-CoV-2 specific primers. Results were expressed as copy number per gram of tissue sample. **(c-d)** Correlation analysis of viral loads measured in lung caudal lobe and PRNT90.

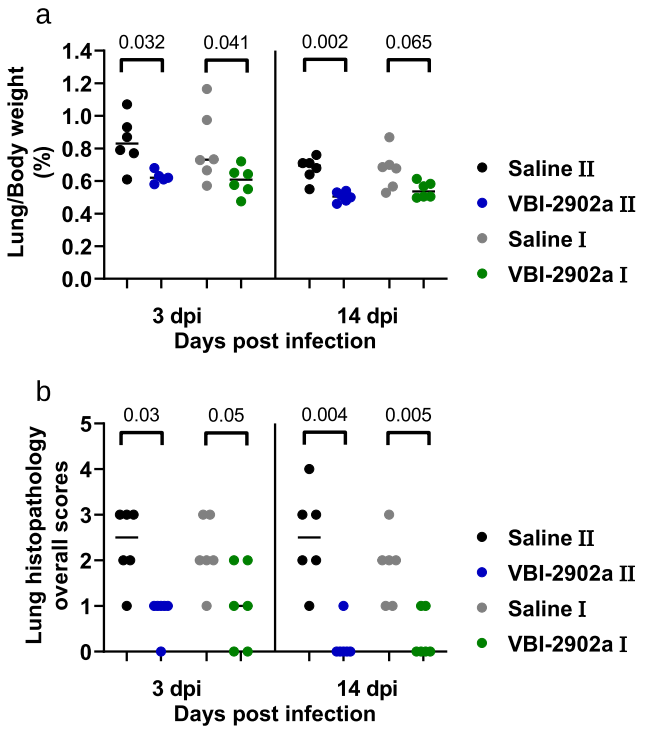

Fig. 9. Clinical evaluation of lung pathology in immunized hamsters challenged by SARS-CoV-2 virus. (a) lung to body weight ratio in hamsters at 3dpi and 14dpi. **(b)** Histopathology severity analysis of hamster lungs at 3dp and 14 dpi. Scores were evaluated on a scale from 0 to 4 as follow: 0, no microscopic lesions; 1, slight or questionable pneumonia; 2, clearly present, but not conspicuously so; 3, moderate pneumonia; 4, severe pneumonia. Statistics were performed using Kruskal-Wallis non-parametric test followed by Dunn' multiple comparisons test. Adjusted p values are shown.

possible is evident as regulatory agencies and vaccine manufactures have discussed the risks and benefits of delaying planned second doses of currently available COVID-19 vaccines to enable immunization of a greater number of individuals as quickly as possible [32,33]. We have previously demonstrated that expression of proteins on the surface of eVLPs dramatically enriches for neutralizing antibody, the presumed correlate of protection against SARS-CoV-2, relative to recombinant proteins [17]. Accordingly, we evaluated different conformations of the SARS-CoV-2 S protein as well as a variety of adjuvants in an effort to identify a COVID-19 vaccine candidate with the potential to confer rapid, robust efficacy.

The eVLPs particles were pseudotyped with SARS-CoV-2 unmodified S protein but expressed low amounts of S that were not suitable for upscaled production. We therefore designed a modified prefusion form of S that resulted in both dramatic increases in yields and enhancement of the nAb response compared to native S. SPG eVLPs induced high titers of RBD Ab binding titers associated with robust neutralizing responses in mice at levels that were much higher than those observed with a recombinant prefusion S protein. Indeed, 14 days after a single dose of SPG eVLPs in Alum, nAb titers exceeded those associated with high titer COVID-19 convalescent sera, persisted and were undiminished for more than 2 months. The potency observed after a single dose of VBI-2902a appears superior to what has been observed after 2 doses in the same strain of mice with an mRNA vaccine that has received Emergency Use Authorization [11,13], further demonstrating the strong potency of this vaccine candidate. In a hamster challenge model VBI-2902a demonstrated robust efficacy against clinical disease and lung inflammation. While two doses showed greater efficacy, a single dose clearly conferred protective benefit.

The value of eVLP expression of the modified SP protein is consistent with prior reports which demonstrated that an anchored version of a stabilized prefusion S antigen provided optimal induction of protective nAbs in Rhesus macaques [12]. Our construct differed from the previously described S-2P [12,34] by using the VSV-G transmembrane cytoplasmic domain to replace that of S, instead of a C-terminal T4 fibritin trimerization domain. Based on previous experience and published data [17,18], we hypothesized that the use of VSV-G tail and expression in the phospholipid membrane of eVLPs would result in natural trimerization of the spike ectodomains providing optimal presentation of neutralization epitopes. The use of the VSV-G tail has been shown to enhance expression and localization of viral glycoproteins at the phospholipid envelop of the particles [35,36].

Aluminum salt adjuvants have a long history of safety and are a component of approved VLP-based vaccines such as Gardasil® against HPV [37] and Engerix B® against HBV [38]. Nevertheless, theoretical concerns have been raised about the use of an aluminum-based adjuvant with a SARS-CoV-2 vaccine and the potential for Th2-mediated enhanced lung pathology [39,40]. Subsequent studies have demonstrated that non-neutralizing antibodies against structural proteins were responsible for the pathology observed in preclinical models [41]. Use of eVLP presentation of an optimized form of the SARS-CoV-2 S protein resulted in a highly potent and focused neutralizing antibody response which avoided any evidence of disease enhancement or increased lung inflammation. In a hamster challenge model VBI-2902a demonstrated efficacy and ability to suppress lung inflammation. While two doses showed better potency, the single dose also conferred protective benefit indicated by comparable results in terms of lung inflammation. Moreover, compared to a clear Th2-biased profile observed in response to recombinant prefusion stabilized S protein in Alum, the similar prefusion S construct induced a balanced Th1/Th2 response when presented by eVLPs. The balanced production of IgG2/IgG1 antibody isotypes after VBI-2902a immunization was comparable with those described in response to the recently emergency use authorized vaccine Ad26.COV2.S [28]. These results emphasize an important difference in the quality of the antibody response when immunizing with soluble, recombinant versus particulate forms of vaccine antigens.

The VBI-2902a vaccine candidate addresses several issues that have thus far hindered the speed and extent of vaccination with currently available COVID-19 vaccines. This includes the need for storage, transport, and distribution of the vaccine at freezing temperatures not typically required for prophylactic vaccines. Indeed, ongoing studies demonstrate that VBI-2902a is stable for at least 6 months at + 2–8 °C (Suppl. Data Fig. 2). This is in line with previous investigations showing 4-year stability of our CMV vaccine candidate VBI-1501 evaluated in phase I clinical trial (NCT02826798). VBI-2902a received approval from Health Canada to initiate its ongoing Phase I/II clinical study (NCT04773665) to assess its potential for one and two dose immunogenicity and potential efficacy in both previously vaccinated and naïve, seronegative individuals.

Funding

VBI-2902a study was supported by Government of Canada Innovation, Science and Industry (ISED) funding through the Strategic Innovation Fund (SIF).

Declaration of Competing Interest

The authors declare the following financial interests/personal relationships which may be considered as potential competing

interests: [Anne-Catherine Fluckiger reports a relationship with VBI Vaccines Inc that includes: consulting or advisory. Barthelemy Ontsouka reports a relationship with VBI Vaccines Inc that includes: employment and equity or stocks. Jasminka Bozic reports a relationship with VBI Vaccines Inc that includes: employment and equity or stocks. Abebaw Diress reports a relationship with VBI Vaccines Inc that includes: employment and equity or stocks. Tanvir Ahmed reports a relationship with VBI Vaccines Inc that includes: employment and equity or stocks. Tamara Berthoud reports a relationship with VBI Vaccines Inc that includes: employment and equity or stocks. Anh Tran reports a relationship with National Research Council Canada that includes: employment. Diane Duque reports a relationship with National Research Council Canada that includes: employment. Liao Mingmin reports a relationship with Vaccine and Infectious Disease Organization International Vaccine Centre that includes: employment. Michael McCluskie reports a relationship with National Research Council Canada that includes: employment. Francisco Diaz-Mitoma reports a relationship with VBI Vaccines Inc that includes: employment and equity or stocks. David E. Anderson reports a relationship with VBI Vaccines Inc that includes: employment and equity or stocks. Catalina Soare reports a relationship with VBI Vaccines Inc that includes: employment and equity or stocks].

Acknowledgement

The authors want to thank Adam Asselin, Matthew Yorke, Teresa Daoud, Lanjian (Isabel) Yang, Rebecca Wang, Gillian Lampkin (VBI vaccines) for outstanding technical support; Traian Sulea (NRC) for discussions on construct design, NRC Animal Resources Group and the VIDO Saskatchewan team for remarkable care with animal experiments as well as Ammon Ding and Echo Wu (Genescript) for their dedication in plasmid preparation. All the people cited above contributed to the success of the study by the excellence of their work.

Appendix A. Supplementary material

Supplementary data to this article can be found online at https://doi.org/10.1016/j.vaccine.2021.07.034.

Reference

[1] Coronavirus Disease (COVID-19) Situation Reports n.d. https://www.who.int/emergencies/diseases/novel-coronavirus-2019/situation-reports.
[2] Calina D, Docea A, Petrakis D, Egorov A, Ishmukhametov A, Gabibov A, et al. Towards effective COVID–19 vaccines: Updates, perspectives and challenges (Review). Int J Mol Med 2020;46:3–16. https://doi.org/10.3892/ijmm.2020.4596.
[3] Li F. Structure, Function, and Evolution of Coronavirus Spike Proteins. Annu Rev Virol 2016;3:237–61. https://doi.org/10.1146/annurev-virology-110615-042301.
[4] Walls AC, Park Y-J, Tortorici MA, Wall A, McGuire AT, Veesler D. Structure, Function, and Antigenicity of the SARS-CoV-2 Spike Glycoprotein. Cell 2020;181:281–292.e6. https://doi.org/10.1016/j.cell.2020.02.058.
[5] Walls AC, Tortorici MA, Snijder J, Xiong X, Bosch B-J, Rey FA, et al. Tectonic conformational changes of a coronavirus spike glycoprotein promote membrane fusion. Proc Natl Acad Sci U S A 2017;114(42):11157–62. https://doi.org/10.1073/pnas.1708727114.
[6] Coutard B, Valle C, de Lamballerie X, Canard B, Seidah NG, Decroly E. The spike glycoprotein of the new coronavirus 2019-nCoV contains a furin-like cleavage site absent in CoV of the same clade. Antiviral Res 2020;176:104742. https://doi.org/10.1016/j.antiviral.2020.104742.
[7] Cai Y, Zhang J, Xiao T, Peng H, Sterling SM, Walsh RM, et al. Distinct conformational states of SARS-CoV-2 spike protein. Science (80-) 2020;369. https://doi.org/10.1126/science.abd4251.
[8] McLellan JS, Chen M, Leung S, Graepel KW, Du X, Yang Y, et al. Structure of RSV fusion glycoprotein trimer bound to a prefusion-specific neutralizing antibody. Science (80-) 2013;340:1113–7. https://doi.org/10.1126/science:1234914.
[9] Pallesen J, Wang N, Corbett KS, Wrapp D, Kirchdoerfer RN, Turner HL, et al. Immunogenicity and structures of a rationally designed prefusion MERS-CoV spike antigen. Proc Natl Acad Sci 2017;114. https://doi.org/10.1073/pnas.1707304114.
[10] Wrapp D, Wang N, Corbett KS, Goldsmith JA, Hsieh C-L, Abiona O, et al. Cryo-EM structure of the 2019-nCoV spike in the prefusion conformation. 2019.
[11] Corbett K, Edwards D, Leist S, Abiona O, Boyoglu-Barnum S, Gillespie R, et al. SARS-CoV-2 mRNA Vaccine Development Enabled by Prototype Pathogen Preparedness. BioRxiv Prepr Serv Biol 2020. https://doi.org/10.1101/2020.06.11.145920.
[12] Mercado NB, Zahn R, Wegmann F, Loos C, Chandrashekar A, Yu J, et al. Single-shot Ad26 vaccine protects against SARS-CoV-2 in rhesus macaques. Nature 2020;586:583–8. https://doi.org/10.1038/s41586-020-2607-z.
[13] Anderson EJ, Rouphael NG, Widge AT, Jackson LA, Roberts PC, Makhene M, et al. Safety and Immunogenicity of SARS-CoV-2 mRNA-1273 Vaccine in Older Adults. N Engl J Med 2020;383:2427–38. https://doi.org/10.1056/NEJMoa2028436.
[14] Walsh EE, Frenck RW, Falsey AR, Kitchin N, Absalon J, Gurtman A, et al. Safety and Immunogenicity of Two RNA-Based Covid-19 Vaccine Candidates. N Engl J Med 2020;383:2439–50. https://doi.org/10.1056/NEJMoa2027906.
[15] Roldão A, Mellado MCM, Castilho LR, Carrondo MJT, Alves PM. Virus-like particles in vaccine development. Expert Rev Vaccines 2010;9:1149–76. https://doi.org/10.1586/erv.10.115.
[16] Bachmann M, Rohrer U, Kundig T, Burki K, Hengartner H, Zinkernagel R. The influence of antigen organization on B cell responsiveness. Science (80-) 1993;262. https://doi.org/10.1126/science.8248784.
[17] Kirchmeier M, Fluckiger A-C, Soare C, Bozic J, Ontsouka B, Ahmed T, et al. Enveloped Virus-Like Particle Expression of Human Cytomegalovirus Glycoprotein B Antigen Induces Antibodies with Potent and Broad Neutralizing Activity. Clin Vaccine Immunol 2014;21. https://doi.org/10.1128/CVI.00662-13.
[18] Garrone P, Fluckiger A-C, Mangeot PE, Gauthier E, Dupeyrot-Lacas P, Mancip J, et al. A Prime-Boost Strategy Using Virus-Like Particles Pseudotyped for HCV Proteins Triggers Broadly Neutralizing Antibodies in Macaques. Sci Transl Med 2011;3. https://doi.org/10.1126/scitranslmed.3002330.
[19] Coronavirus Disease 2019 (COVID-19) Treatment Guidelines. n.d.
[20] Côté J, Garnier A, Massie B, Kamen A. Serum-free production of recombinant proteins and adenoviral vectors by 293SF-3F6 cells. Biotechnol Bioeng 1998;59:567–75.
[21] Ou X, Liu Y, Lei X, Li P, Mi D, Ren L, et al. Characterization of spike glycoprotein of SARS-CoV-2 on virus entry and its immune cross-reactivity with SARS-CoV. Nat Commun 2020;11. https://doi.org/10.1038/s41467-020-15562-9.
[22] Sun Z, Ren K, Zhang X, Chen J, Jiang Z, Jiang J, et al. Mass Spectrometry Analysis of Newly Emerging Coronavirus HCoV-19 Spike Protein and Human ACE2 Reveals Camouflaging Glycans and Unique Post-Translational Modifications. Engineering 2020. https://doi.org/10.1016/j.eng.2020.07.014.
[23] Kittel M, Muth MC, Zahn I, Roth H-J, Thiaucourt M, Gerhards C, et al. Clinical evaluation of commercial automated SARS-CoV-2 immunoassays. Int J Infect Dis 2021;103:590–6. https://doi.org/10.1016/j.ijid.2020.12.003.
[24] Ni L, Ye F, Cheng M-L, Feng Yu, Deng Y-Q, Zhao H, et al. Detection of SARS-CoV-2-Specific Humoral and Cellular Immunity in COVID-19 Convalescent Individuals. Immunity 2020;52. https://doi.org/10.1016/j.immuni.2020.04.023.
[25] Cubas R, Zhang S, Kwon S, Sevick-Muraca EM, Li M, Chen C, et al. Virus-like Particle (VLP) Lymphatic Trafficking and Immune Response Generation After Immunization by Different Routes. J Immunother 2009;32. https://doi.org/10.1097/CJI.0b013e31818f13c4.
[26] Peeples L. News Feature: Avoiding pitfalls in the pursuit of a COVID-19 vaccine. Proc Natl Acad Sci 2020;117. https://doi.org/10.1073/pnas.2005456117.
[27] Roncati L, Nasillo V, Lusenti B, Riva G. Signals of Th2 immune response from COVID-19 patients requiring intensive care. Ann Hematol 2020;99. https://doi.org/10.1007/s00277-020-04066-7.
[28] Bos R, Rutten L, van der Lubbe JEM, Bakkers MJG, Hardenberg G, Wegmann F, et al. Ad26 vector-based COVID-19 vaccine encoding a prefusion-stabilized SARS-CoV-2 Spike immunogen induces potent humoral and cellular immune responses. npj Vaccines 2020;5. https://doi.org/10.1038/s41541-020-00243-x.
[29] Chan JF-W, Zhang AJ, Yuan S, Poon VK-M, Chan CC-S, Lee AC-Y, et al. Simulation of the Clinical and Pathological Manifestations of Coronavirus Disease 2019 (COVID-19) in a Golden Syrian Hamster Model: Implications for Disease Pathogenesis and Transmissibility. Clin Infect Dis 2020. https://doi.org/10.1093/cid/ciaa325.
[30] Sia SF, Yan L-M, Chin AWH, Fung K, Choy K-T, Wong AYL, et al. Pathogenesis and transmission of SARS-CoV-2 in golden hamsters. Nature 2020;583(7818):834–8. https://doi.org/10.1038/s41586-020-2342-5.
[31] Roberts A, Vogel L, Guarner J, Hayes N, Murphy B, Zaki S, et al. Severe Acute Respiratory Syndrome Coronavirus Infection of Golden Syrian Hamsters. J Virol 2005;79(1):503–11. https://doi.org/10.1128/JVI.79.1.503-511.2005.
[32] https://www.fda.gov/news-events/press-announcements/fda-statement-following-authorized-dosing-schedules-covid-19-vaccines n.d.
[33] WHO-2019-nCoV-vaccines-SAGE_recommendation-BNT162b2-2021.1-eng n.d.
[34] Kuo T-Y, Lin M-Y, Coffman RL, Campbell JD, Traquina P, Lin Y-J, et al. Development of CpG-adjuvanted stable prefusion SARS-CoV-2 spike antigen as a subunit vaccine against COVID-19. Sci Rep 2020;10. https://doi.org/10.1038/s41598-020-77077-z.
[35] Schnell MJ, Buonocore L, Kretzschmar E, Johnson E, Rose JK. Foreign glycoproteins expressed from recombinant vesicular stomatitis viruses are incorporated efficiently into virus particles. Proc Natl Acad Sci 1996;93. https://doi.org/10.1073/pnas.93.21.11359.

[36] Nègre D, Mangeot P-E, Duisit G, Blanchard S, Vidalain P-O, Leissner P, et al. Characterization of novel safe lentiviral vectors derived from simian immunodeficiency virus (SIVmac251) that efficiently transduce mature human dendritic cells. Gene Ther 2000;7(1). https://doi.org/10.1038/sj.gt.3301292.
[37] Muñoz N, Manalastas R, Pitisuttithum P, Tresukosol D, Monsonego J, Ault K, et al. Safety, immunogenicity, and efficacy of quadrivalent human papillomavirus (types 6, 11, 16, 18) recombinant vaccine in women aged 24–45 years: a randomised, double-blind trial. Lancet 2009;373. https://doi.org/10.1016/S0140-6736(09)60691-7.
[38] Keating GM, Noble S. Recombinant Hepatitis B Vaccine (Engerix-B??). Drugs 2003;63. https://doi.org/10.2165/00003495-200363100-00006.
[39] Tseng C-T, Sbrana E, Iwata-Yoshikawa N, Newman PC, Garron T, Atmar RL, et al. Immunization with SARS Coronavirus Vaccines Leads to Pulmonary Immunopathology on Challenge with the SARS Virus. PLoS One 2012;7. https://doi.org/10.1371/journal.pone.0035421.
[40] Eichinger KM, Kosanovich JL, Gidwani SV, Zomback A, Lipp MA, Perkins TN, et al. Prefusion RSV F Immunization Elicits Th2-Mediated Lung Pathology in Mice When Formulated With a Th2 (but Not a Th1/Th2-Balanced) Adjuvant Despite Complete Viral Protection. Front Immunol 2020;11. https://doi.org/10.3389/fimmu.2020.01673.
[41] Yasui F, Kai C, Kitabatake M, Inoue S, Yoneda M, Yokochi S, et al. Prior Immunization with Severe Acute Respiratory Syndrome (SARS)-Associated Coronavirus (SARS-CoV) Nucleocapsid Protein Causes Severe Pneumonia in Mice Infected with SARS-CoV. J Immunol 2008;181(9):6337–48. https://doi.org/10.4049/jimmunol.181.9.6337.